synchrotron or inverse Compton emission from the jet already observed in the radio band (*23*). Unfortunately, current knowledge of the jet at radio wavelengths does not allow discriminating between the two processes.

To have such a clear polarimetric signal, the magnetic field has to be coherent over a large fraction of the emission site (*5*). Such a coherent magnetic-field structure may indicate a jet origin for the gamma rays above 400 keV (*24*). In addition, because the gamma rays emitted in BH x-ray binaries are generally thought to be emitted close to the BH horizon (*7*, *25*), and because the synchrotron photons we observed in the hard tail are too energetic to be effectively self-Comptonized, these observations might be evidence that the jet structure is formed in the BH vicinity, possibly in the Compton corona itself. Another possibility is that the gamma rays are produced in the initial acceleration region in the jet, as observed at higher energies by the Fermi Large Area Telescope from the microquasar Cygnus X-3 (*26*).

The spectrum observed above 400 keV is consistent with a power law of photon index 1.6 ± 0.2. This means that this spectrum, if due to synchrotron or inverse Compton emission, is caused by electrons whose energy distribution is also a power law with an index p of 2.2 ± 0.4 (*27*), consistent with the canonical value for shock-accelerated particles $p = 2$. Synchrotron radiation at MeV energies implies also that the electron energy, for a magnetic field of 10 mG, which is reasonable for this kind of system (*28*), would be around a few TeV (*27*, *29*). Inverse Compton scattering of photons off these high-energy TeV electrons, whose lifetime due to synchrotron energy loss is about 1 month (*27*), could also be the origin of the TeV photons detected from Cygnus X-1 with the Major Atmospheric Gamma-ray Imaging Cerenkov telescope experiment (*30*) and possibly also the gamma rays claimed by Astrorivelatore Gamma ad Immagini Leggero/Light Imager for Gamma-Ray Astrophysics (*31*).

The position angle (PA) of the electric vector, which gives the direction of the electric field lines projected onto the sky, is $140° \pm 15°$. This is at least $100°$ away from the compact radio jet, which is observed at a PA of $21°$ to $24°$ (*32*). Such deviations between the electric field vector and jet direction are also found in other jet sources, such as Active Galactic Nuclei (*33*) or the galactic source SS433 (*34*).

References and Notes

1. R. A. Sunyaev, J. Trümper, *Nature* **279**, 506 (1979).
2. M. Gierliński *et al.*, *Mon. Not. R. Astron. Soc.* **288**, 958 (1997).
3. A. M. Stirling *et al.*, *Mon. Not. R. Astron. Soc.* **327**, 1273 (2001).
4. R. P. Fender *et al.*, *Mon. Not. R. Astron. Soc.* **369**, 603 (2006).
5. E. Gallo, R. P. Fender, G. G. Pooley, *Mon. Not. R. Astron. Soc.* **344**, 60 (2003).
6. W. Cui *et al.*, *Astrophys. J.* **474**, L57 (1997).
7. T. Di Salvo, C. Done, P. T. Życki, L. Burderi, N. R. Robba, *Astrophys. J.* **547**, 1024 (2001).
8. K. Ebisawa, Y. Ueda, H. Inoue, Y. Tanaka, N. E. White, *Astrophys. J.* **467**, 419 (1996).
9. M. L. McConnell *et al.*, *Astrophys. J.* **572**, 984 (2002).
10. M. Cadolle Bel *et al.*, *Astron. Astrophys.* **446**, 591 (2006).
11. P. Massey, K. E. Johnson, K. Degioia-Eastwood, *Astrophys. J.* **454**, 151 (1995).
12. D. R. Gies, C. T. Bolton, *Astrophys. J.* **304**, 371 (1986).
13. M. Bałucińska-Church, T. Belloni, M. J. Church, G. Hasinger, *Astron. Astrophys.* **302**, L5 (1995).
14. G. Vedrenne *et al.*, *Astron. Astrophys.* **411**, L63 (2003).
15. P. Ubertini *et al.*, *Astron. Astrophys.* **411**, L131 (2003).
16. C. Winkler *et al.*, *Astron. Astrophys.* **411**, L1 (2003).
17. F. Lei, A. J. Dean, G. L. Hills, *Space Sci. Rev.* **82**, 309 (1997).
18. M. Forot, P. Laurent, F. Lebrun, O. Limousin, *Astrophys. J.* **668**, 1259 (2007).
19. M. Forot, P. Laurent, I. A. Grenier, C. Gouiffès, F. Lebrun, *Astrophys. J.* **688**, L29 (2008).
20. D. Götz, P. Laurent, F. Lebrun, F. Daigne, Ž. Bošnjak, *Astrophys. J.* **695**, L208 (2009).
21. In brief, a Compton polarimeter uses the polarization dependency of the differential cross section for Compton scattering, where linearly polarized photons scatter preferentially perpendicularly to the incident polarization vector. By examining the scatter-angle azimuthal distribution of the detected photons, a sinusoidal signal is obtained from which the PA and the Pf with respect to a 100% polarized source can be derived. Gamma-ray polarization measurements are particularly difficult, the main difficulty being the exclusion of systematic/detector effects in the azimuthal Compton events distribution. To exclude these systematic effects, we followed the process detailed in (*19*). We only considered events that interacted once in the upper CdTe crystal layer, Integral Soft Gamma-Ray Imager (sensitive in the 15- to 1000-keV band), and once in the lower CsI layer, Pixelated CsI Telescope (sensitive in the 200-keV to 10-MeV band), and whose reconstructed energy was in the 250- to 2000-keV energy range. These events were automatically selected on board through a time coincidence algorithm. The maximal allowed time window was set to 3.8 µs during our observations, which span between 2003 and 2009, for a total exposure of more than 5 million seconds, which is ~58 days.
22. R. A. Sunyaev, L. Titarchuk, *Astrophys. J.* **143**, 374 (1985).
23. R. P. Fender, T. Belloni, E. Gallo, *Mon. Not. R. Astron. Soc.* **355**, 1105 (2004).
24. J. F. Hawley, *Astrophys. Space Sci.* **320**, 107 (2009).
25. J. B. Dove, J. Wilms, M. Maisack, M. C. Begelman, *Astrophys. J.* **487**, 759 (1997).
26. A. A. Abdo *et al.*; Fermi LAT Collaboration, *Science* **326**, 1512 (2009).
27. V. L. Ginzburg, S. I. Syrovatskii, *Annu. Rev. Astron. Astrophys.* **3**, 297 (1965).
28. L. F. Rodriguez, I. F. Mirabel, *Astrophys. J.* **511**, 398 (1999).
29. In the inverse Compton case, electrons will be of much lower energies.
30. J. Albert *et al.*, *Astrophys. J.* **665**, L51 (2007).
31. S. Sabatini *et al.*, *Astrophys. J.* **712**, L10 (2010).
32. This compact radio jet PA value is slightly time dependent (*3*).
33. M. L. Lister, D. C. Homan, *Astron. J.* **130**, 1389 (2005).
34. M. C. Begelman, A. R. King, J. E. Pringle, *Mon. Not. R. Astron. Soc.* **370**, 399 (2006).

Selective, Nickel-Catalyzed Hydrogenolysis of Aryl Ethers

Alexey G. Sergeev and John F. Hartwig*

Selective hydrogenolysis of the aromatic carbon-oxygen (C-O) bonds in aryl ethers is an unsolved synthetic problem important for the generation of fuels and chemical feedstocks from biomass and for the liquefaction of coal. Currently, the hydrogenolysis of aromatic C-O bonds requires heterogeneous catalysts that operate at high temperature and pressure and lead to a mixture of products from competing hydrogenolysis of aliphatic C-O bonds and hydrogenation of the arene. Here, we report hydrogenolyses of aromatic C-O bonds in alkyl aryl and diaryl ethers that form exclusively arenes and alcohols. This process is catalyzed by a soluble nickel carbene complex under just 1 bar of hydrogen at temperatures of 80 to 120°C; the relative reactivity of ether substrates scale as Ar-OAr>>Ar-OMe>ArCH₂-OMe (Ar, Aryl; Me, Methyl). Hydrogenolysis of lignin model compounds highlights the potential of this approach for the conversion of refractory aryl ether biopolymers to hydrocarbons.

Selective hydrogenolysis of aromatic carbon-oxygen (C-O) bonds (scission by reaction with hydrogen to form CH and OH bonds in their place) is challenging because of the strength and stability of these linkages (*1*); yet, this process is important for the conversion of oxygen-rich lignocellulosic plant biomass to de-

oxygenated fuels and commercial chemicals (*2–5*). Whereas the exclusively aliphatic C-O bonds in cellulose can be cleaved with hydrolysis and dehydration (*3*), the aromatic C-O bonds in lignin cannot undergo these processes and have resisted selective cleavage by hydrogen (*2*, *4*). In addition, brown coal's polymeric network contains aromatic C-O bonds inherited from lignocellulosic biomass, and the liquefaction of these bonds could facilitate the liquification of this carbon source and its conversion to arene feedstocks (*6*). A general, mild method for reductive cleav-

Department of Chemistry, University of Illinois, 600 South Matthews Avenue, Urbana, IL 61801, USA.

*To whom correspondence should be addressed. E-mail: jhartwig@illinois.edu

age of unactivated aromatic C-O bonds would furthermore expand the utility of alkoxy and aryloxy substituents as removable directing groups (*7*) that can influence synthetic transformations of aromatic systems.

In contrast to hydrogenolysis of benzyl ethers, which proceeds selectively under mild conditions over heterogeneous catalysts (*8*), the cleavage of C-O bonds in aryl ethers requires high temperatures and pressures (over 250°C and 30 bar) and occurs with poor selectivities (*1, 2*); typical product mixtures include saturated cyclic hydrocarbons and cycloalkanols from hydrogenation of the arene rings and concurrent aliphatic C-O bond cleavage (*1, 2, 9–12*). This arene reduction wastes hydrogen and renders the reaction less useful for producing aromatic feedstocks (*2, 4*). Alternative methods for the cleavage of aryl ethers that avoid this side reaction require stoichiometric alkali metals (*13*) or electrocatalytic hydrogenolysis (*14*), both of which are expensive and difficult to conduct on a large scale. Here, we report the selective, reductive cleavage of various aromatic C-O bonds with hydrogen catalyzed by a single soluble nickel catalyst under mild conditions (*15*). Hydrogenolysis with this catalyst proceeds without concurrent arene ring hydrogenation and reduction of aliphatic C-O bonds.

To realize a selective hydrogenolysis of aromatic C-O bonds, we envisioned a reaction that involves insertion of a discrete transition metal complex into the aromatic C-O bond and reaction of the resulting intermediate with hydrogen to yield arene and alcohol. We anticipated that the low reactivity of homogeneous catalysts toward hydrogenation of aromatic rings (*16*) would prevent competitive formation of cycloalkanes and cycloalkanols from such a process. Nickel complexes known to activate aromatic C-O bonds in the presence of aliphatic C-O bonds (*17–21*) were the starting point for our catalyst development.

Catalytic reactions involving aromatic C-O bond cleavage with nickel complexes were first reported by Wenkert for cross-coupling of aryl ethers with Grignard reagents to form biaryl compounds (*17, 18*). This reactivity has been developed further in recent years with less aggressive carbon nucleophiles and improved catalysts (*19–21*). However, the extension of such reactivity to the hydrogenolysis of C-O bonds is challenging because hydrogen is less reactive than main group carbon nucleophiles, and the hydrogenolysis or hydrogenation of typically unreactive moieties can lead to reduction of the catalyst itself to form
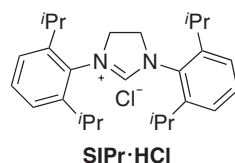
heterogeneous systems (*22*) that are less selective than their homogeneous counterparts. Indeed, our initial attempts to conduct the hydrogenolysis of aryl C-O bonds in diphenyl ether at 120°C under 1 bar of hydrogen with 20 mole percent (mol %) of the nickel catalyst generated from Ni(COD)$_2$ (COD, 1,5-cyclooctadiene) and PCy$_3$ (Cy, cyclohexyl), which was used previously for cross-couplings (*19–21*), led to very low conversion of the ether (~1%) (fig. S1) (*23*). Cyclohexane and cyclohexene were formed under these conditions, implying that cleavage of the C-P bond in the phosphine ligand to form these products leads to decomposition of the catalyst (*24*).

Thus, we evaluated a series of nickel catalysts containing *N*-heterocyclic carbenes (NHCs) as the dative ligands. *N*-Heterocyclic carbenes typically bind late-transition metal centers more tightly than do phosphines (*25, 26*) and lack labile P-C bonds. The stronger metal-ligand bonds would discourage formation of heterogeneous nickel. We initially tested nickel-NHC catalysts for the reduction of the C-O bond of diphenyl ether in the presence of the hydride donors, DIBALH (di*iso*butylaluminum hydride), LiAl(O^{t}Bu)$_3$H,

and Et$_3$SiH in place of H$_2$ because of the convenience of evaluating catalysts for reactions with liquid and solid reagents. These reactions were conducted with the combination of a nickel(0) precursor, Ni(COD)$_2$ or Ni(acac)$_2$ (acac, acetylacetonate), and an NHC ligand formed in situ through deprotonation of the corresponding salt NHC·HX with a base (NaO^{t}Bu) (table S1). We found that high yields of the products from aromatic C-O bond cleavage were obtained with Ni(COD)$_2$ as the source of nickel, SIPr·HCl (fig. 1) as ligand precursor, and the aluminum hydrides DIBALH and LiAl(O^{t}Bu)$_3$H (2.5 equiv.) as reducing agents in the presence of an excess of NaO^{t}Bu (2.5 equiv.) as a base in toluene (tables S1 and S2). These initial studies showed that the single Ni(0)–NHC system, in tandem with either aluminum hydrides or silane-reducing agents, catalyzes the reductive cleavage of the aromatic C-O bonds of unactivated aryl ethers in diaryl ethers and alkyl aryl ethers, as well as the benzylic C-O bonds in benzyl aryl ethers and benzyl alkyl ethers (table S2) (*27*).

Having identified Ni(0)–NHC complexes as unusually active catalysts for the cleavage of a

Table 1. Hydrogenolysis of diaryl ethers. The reactions were conducted in closed glass reaction vessels filled with hydrogen at 1 bar gauge pressure at 24°C. After the time listed, no further changes in conversion were observed. The yields of arenes and phenols formed by the bond cleavage shown were measured with gas chromatography after acidification and aqueous work up.

Entry	Diaryl ether	Ni, mol%	T, °C	Time, h	Conversion, %	Arene, %	Phenol, %
1		20	120	16	100	99	99
2		10	120	32	87	82	87
3		5	120	32	59	59	54
4	Me / Me	20	120	16	100	96	99
5	MeO / OMe	20	120	16	94	88*	86†
6	Me / Me	20	120	48	100	97	99
7	^{t}Bu / ^{t}Bu	20	120	48	74	72	73
8	F$_3$C	10	100	16	100	87§	99
9	F$_3$C / OMe	10	100	16	100	87‖	92
10	/ OMe	20	120	16	100	88¶	80#
11	Me / Me	20	120	32	85	85	85

Reaction scheme: Diaryl ether (R^1, R^2 substituted) + H$_2$ (1 bar) → [5-20% Ni(COD)$_2$, 10-40% SIPr·HCl, NaO^{t}Bu, *m*-xylene, Temp, Time] → arene (R^1) + HO-phenol (R^2)

*Anisole (65%) and benzene (23%). †3-Methoxyphenol (83%) and phenol (3%). ‡Trifluoromethylbenzene (64%) and toluene (23%); benzene (4%) as a side product. §Trifluoromethylbenzene (68%) and toluene (19%). ‖Anisole (4%) as a side product. ¶Phenol (17%) as a side product.

Fig. 1. A *N*-Heterocyclic carbene ligand precursor used in the study. (SIPr·HCl)

range of aryl and benzyl ethers with main group hydride donors, we explored the use of hydrogen—a cheaper, cleaner, and milder reagent—for the reduction of aryl ethers (tables S3 and S4). Indeed, the combination of Ni(COD)$_2$ and SIPr·HCl (20 mol %) as catalyst and NaO^{t}Bu (2.5 equiv.) as base effected the selective hydrogenolysis of various diaryl ethers with only 1 bar pressure of H$_2$ in *m*-xylene to give the corresponding arenes and phenols in good to excellent yields (Table 1). The scope of the reaction encompasses both electron-rich and electron-poor diaryl ethers. Hydrogenolysis occurred faster with unsubstituted diphenyl ether and diaryl ethers bearing an electron-withdrawing trifluoromethyl group (Table 1, entries 1, 2, 8, and 9) than with diaryl ethers bearing electron-donating alkyl or methoxy substituents. Reactions with the less reactive diaryl ethers required substantial catalyst loadings (20%) but occurred to high conversions (Table 1, entries 4 to 7). Unsymmetrical diaryl ethers were cleaved preferentially at the C–O bond adjacent to the more electron-poor aryl ring, as shown in Table 1, entries 8 to 10. The sterically hindered substrate di-2-tolyl ether also underwent hydrogenolysis to give toluene and *o*-cresol in 85% yields (Table 1, entry 11). No detectable products from hydrogenation of the arene ring were observed in any of the experiments. As noted earlier, this complete selectivity for reduction of the C–O bonds over the aryl π-bonds contrasts with that for hydrogenation of aryl ethers over heterogeneous catalysts, which typically leads to a mixture of arenes, cycloalkanes, phenols, and cycloalkanols (*1*, *2*, *9*–*12*).

The nickel catalyst is also active under comparable conditions for the selective hydrogenolysis of aryl alkyl ethers to form arenes and aliphatic alcohols (Table 2). For example, the hydrogenolyses of 1-methoxynaphthalene, 2-alkoxynaphthalenes, and 4-alkoxybiphenyls under 1 bar of H$_2$ in *m*-xylene at 120°C led to the corresponding arenes in 59 to 95% yields in the presence of 20 mol % of Ni(COD)$_2$ and SIPr·HCl as catalyst and NaO^{t}Bu as a base (Table 2). In these cases, at least 95% of the consumed aryl ether was converted to the corresponding arene. The amount of aliphatic alcohol formed from reactions of aryl *n*-hexyl ethers was quantified after conversion to the trimethylsilyl ether, and *n*-hexanol was shown to be formed in high yield (Table 2, entries 1 and 6). Hydrogenolyses of 1- and 2-methoxynaphthalene proceeded to full conversion to form the arene in nearly quantitative 99 and 98% yields in the presence of the Lewis acid AlMe$_3$ at 100°C and 80°C, respectively (Table 2, entries 3 and 5); no considerable improvement in the yield of arene, however, was observed for the hydrogenolysis of 4-methoxybiphenyl in the presence of the Lewis acid (Table 2, entry 8). In no case did we observe any products from aliphatic C–O bond cleavage; products of arene hydrogenation were, again, detected only in trace amounts (<2%). In contrast, the hydrogenolysis of 2-methoxynaphthalene over Raney Nickel has been shown previously to form 1,2,3,4-tetrahydronaphthalene and 6-methoxy-1,2,3,4-tetrahydronaphthalene under acidic and basic conditions, respectively (*12*).

The Ni-SIPr system also catalyzed the hydrogenolysis of benzyl aryl ethers under 1 bar of H$_2$ in *m*-xylene at 120°C (Table 3, entry 1). In contrast, benzyl alkyl ethers such as 4-*tert*-butylbenzyl methyl ether and α-ethylbenzyl methyl ether were completely resistant to hydrogenolysis under conditions that led to the cleavage of diaryl and benzyl alkyl ethers (120°C, 16 hours), as shown in Table 3, entries 2 and 4. These results are intriguing because such benzyl alkyl ethers are known to be labile toward hydrogenolysis at the C–O bonds in the presence of heterogeneous catalysts (*8*). Alkyl benzyl ether can nevertheless be cleaved in excellent yields in the presence of the Ni-SIPr system and 1 equiv. of AlMe$_3$ as an additive at 120°C (Table 3, entries 3 and 5) (*28*).

The broad substrate scope of hydrogenolysis by the Ni-SIPr system prompted us to estimate the relative rates for cleavage of diaryl, alkyl aryl, and benzyl alkyl ethers by conducting competition experiments in which two substrates are present in the same vessel, allowing further comparisons to typical heterogeneous catalysts. Consistent with the reactivity of the different ethers in separate reactions, diphenyl ether was cleaved in complete preference to a benzyl alkyl ether under 1 bar of hydrogen in *m*-xylene with 20 mol % of the Ni-SIPr catalyst and NaO^{t}Bu as base. Quantitative yields of benzene and phenol were observed after 16 hours at 120°C (Fig. 2B). Likewise, reduction of the aromatic C–O bond in an alkyl aryl ether occurred in the presence of the benzylic C–O bond in an alkyl benzyl ether in the presence or absence of AlMe$_3$ (Fig. 2C). Again, these relative rates contrast sharply with those of heterogeneous systems that cleave benzylic C–O bonds faster than aromatic C–O bonds (*29*). Lastly, hydrogenolysis of diphenyl ether occurred preferentially over hydrogenolysis of 4-*tert*-butylphenyl methyl ether (100:5) (Fig. 2D), leading to the overall relative reactivities shown in Fig. 2A.

To probe whether the Ni-NHC system reacts as a homogeneous catalyst or generates a heterogeneous catalyst that reacts with unusual se-

Table 2. Hydrogenolysis of alkyl aryl ethers.

$$R\text{-}C_6H_4\text{-OAlk} + H_2 \ (1 \text{ bar}) \xrightarrow[\text{NaO}^t\text{Bu, }m\text{-xylene, Temp, 16 h}]{20\% \ \text{Ni(COD)}_2, \ 40\% \ \text{SIPr·HCl}} R\text{-}C_6H_5 + \text{AlkOH}$$

Entry	Alkyl Aryl Ether		T, °C	Time, h	Additive (1 equiv.)	Conversion, %	Arene, %	AlkOH, %
1	2-naphthyl-OAlk	Alk = ^{n}Hexyl	120	16	-	100	95	98
2		Alk = Methyl	120	16	-	89	89	nq*
3		Alk = Methyl	80	16	AlMe$_3$	100	98	nq
4	1-naphthyl-OMe		120	16	-	72	72	nq
5			100	16	AlMe$_3$	100	99	nq
6	Ph-C$_6$H$_4$-OAlk	Alk = ^{n}Hexyl	120	32	-	85	85	85
7		Alk = Methyl	120	32	-	60	59	nq
8		Alk = Methyl	100	32	AlMe$_3$	65	65	nq

*nq, not quantified.

Table 3. Hydrogenolysis of benzyl ethers.

$$R^1\text{-}C_6H_4\text{-CH(OR}^2)R^3 + H_2 \ (1 \text{ bar}) \xrightarrow[\text{NaO}^t\text{Bu, }m\text{-xylene, 120 °C, 16h}]{20 \ \text{mol\% Ni(COD)}_2, \ 40 \ \text{mol\% SIPr·HCl}} R^1\text{-}C_6H_4\text{-CH}_2R^3 + R^2\text{OH}$$

Entry	Alkyl Benzyl Ether	Ni, mol%	Additive (1 equiv.)	Conversion, %	Arene, %	R^{2}OH, %
1	4-^{t}Bu-benzyl-OPh	10	-	100	99	93
2	4-^{t}Bu-benzyl-OMe	20	-	1	0	0
3	4-^{t}Bu-benzyl-OMe	20	AlMe$_3$	100	99	nq*
4	benzyl(Et)-OMe	20	-	0	0	0
5	benzyl(Et)-OMe	20	AlMe$_3$	100†	96	nq

*nq, not quantified. †32 hours.

lectivity, we conducted the hydrogenolysis of diphenyl ether and 2-methoxynaphthalene in the presence of a 300-fold excess of mercury with respect to the catalyst. No decrease in conversion or product yields was observed (*23*). Although such data are suggestive, rather than fully conclusive, of the homogeneity versus heterogeneity of the catalyst, the absence of poisoning by mercury is consistent with our proposal that the distinct selectivities result from the action of a homogeneous catalyst (*22*).

Having identified a catalyst for the reductive cleavage of simple diaryl ethers, we tested the ability of this system to catalyze the hydrogenol-ysis of an oligomeric aryl ether. Hydrogenolysis of the oligomeric phenylene oxide containing eight aromatic C-O bonds (Fig. 3A) in the presence of 10 mol % of the catalyst per C-O bond under 1 bar of hydrogen at 120°C in *m*-xylene resulted in complete depolymerization to give benzene, phenol, and resorcinol in good total yield.

Lastly, we studied the hydrogenolysis of various aromatic and benzylic C-O bonds that constitute roughly 75% of all the intermonomer linkages in lignin, one of the most stable bio-polymers in nature (Fig. 3, B to D) (*2*, *5*). Cleavage of each of these ether linkages with a single catalyst would illustrate the potential to conduct the catalytic depolymerization and valorization of lignin to form aromatic products (*4*). The diaryl ether models of one of the most recalcitrant lignin linkages, the 4-O-5 linkage, were cleaved under 1 bar of hydrogen at 120°C in *m*-xylene to yield anisole, benzene, and phenols in moderate yields in the presence of 20 mol % of the catalyst generated from Ni(COD)$_2$ and SIPr·HCl (Fig. 3B). Hydrogenolysis of the α-O-4 lignin model compound proceeded with just 5 mol % of the Ni-SIPr catalyst at 80°C under 1 bar of hydrogen to afford 3,4-dimethoxytoluene and 2-methoxyphenol in nearly quantitative yields (Fig. 3C). In agreement with previous results, cleavage of the β-O-4 model under the basic conditions of our system proceeded without catalyst to give guaiacol in 89% yield (Fig. 3D) (*30*).

Available data do not allow one to distinguish between several possible mechanisms for the nickel-catalyzed hydrogenolysis of aryl ethers, but several mechanisms can be envisioned. The nickel center that cleaves the aromatic C-O bond could be a nickel hydride, a neutral nickel(0) complex, or an anionic nickelate species. The favorable effect of the strong base in the hydrogenolysis could lead to the formation of anionic nickel complexes that are more active for the cleavage of the C-O bonds or for activation of coordinated dihydrogen. Although these mechanistic issues are yet to be resolved, and turnover numbers of the catalyst must be improved, the results from this work have demonstrated that the selective cleavage of aromatic C-O bonds in the presence of other C-O bonds can be conducted without reduction of the arene units by using a widely available metal and the cheap, mild, and atom-economical reductant hydrogen.

Fig. 2. (**A**) Relative reactivity of aryl and benzyl ethers toward hydrogenolysis of C-O bonds catalyzed by Ni(COD)$_2$ and SIPr. Selective hydrogenolysis of (**B**) diphenyl ether in the presence of 4-*tert*-butylbenzyl methyl ether; (**C**) 2-methoxynaphthalene in the presence of 4-*tert*-butylbenzyl methyl ether; and (**D**) diphenyl ether in the presence of 4-*tert*-butylanisole.

Fig. 3. Hydrogenolysis of (**A**) bis(*m*-phenoxyphenyl)benzene. (**B**) A model of the 4-O-5 linkage in lignin. (**C**) A model of the α–O-4 linkage in lignin. (**D**) A model of the β–O-4 linkage in lignin.

References and Notes
1. E. Furimsky, *Appl. Catal. A.* **199**, 147 (2000).
2. J. Zakzeski, P. C. A. Bruijnincx, A. L. Jongerius, B. M. Weckhuysen, *Chem. Rev.* **110**, 3552 (2010).
3. G. W. Huber, S. Iborra, A. Corma, *Chem. Rev.* **106**, 4044 (2006).
4. A. L. Marshall, P. J. Alaimo, *Chem. Eur. J.* **16**, 4970 (2010).
5. Y. Pu, D. Zhang, P. M. Singh, A. J. Ragauskas, *Biofuels Bioprod. Bioref.* **2**, 58 (2008).
6. D. G. Levine, R. H. Schlosenberg, B. G. Silbernagel, *Proc. Natl. Acad. Sci. U.S.A.* **79**, 3365 (1982).
7. We define a directing group as a substituent, usually containing a basic heteroatom, attached to the aromatic ring that enables functionalization of the arene by
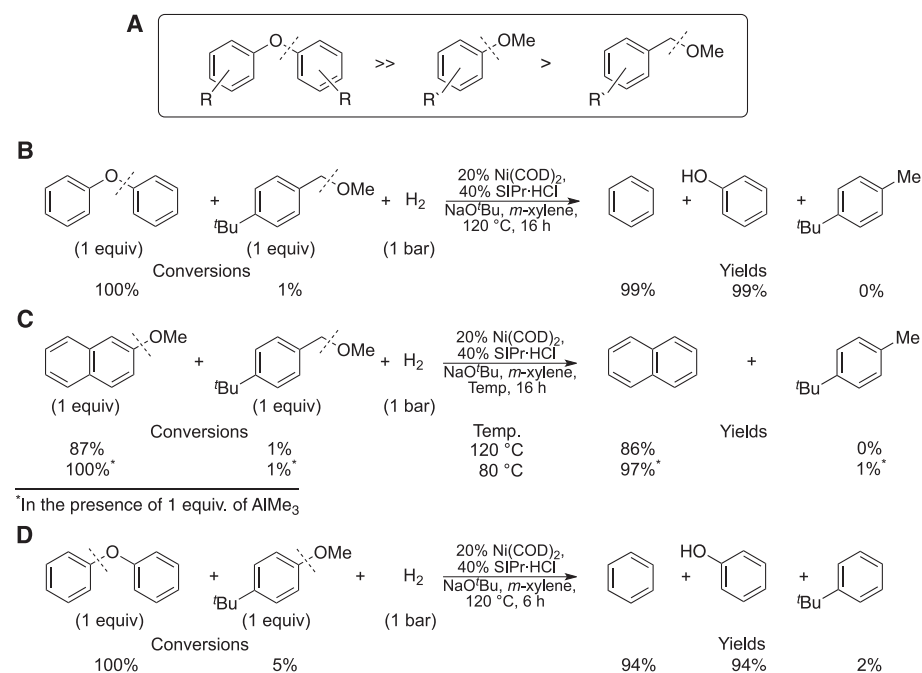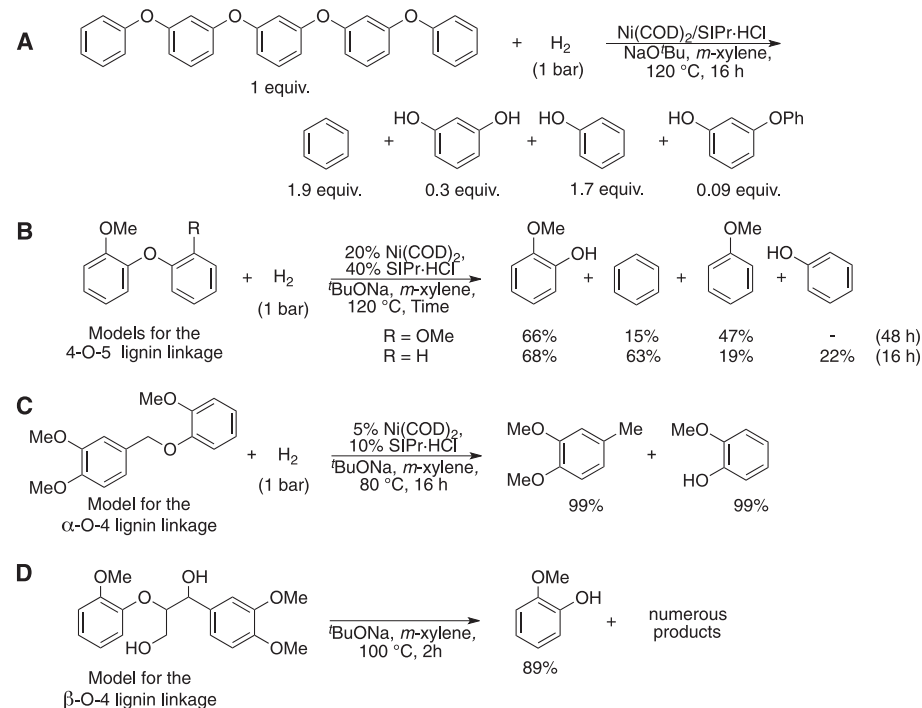
reaction of an organometallic reagent at a specific position, usually ortho to the directing group, followed by the reaction of the metallated aromatic compound with an electrophile. For application of these groups in directed *ortho*-lithiation see (*31*).

8. P. N. Rylander, *Hydrogenation Methods* (Academic Press, London, 1985), pp. 157–163.
9. M. K. Huuska, *Polyhedron* **5**, 233 (1986).
10. S. Utoh, T. Hirata, H. Oda, C. Yokokawa, *Fuel Proc. Tech.* **14**, 221 (1986).
11. E. M. Van Duzee, H. Adkins, *J. Am. Chem. Soc.* **57**, 147 (1935).
12. G. Stork, *J. Org. Chem.* **69**, 576 (1947).
13. A. Maercker, *Angew. Chem. Int. Ed. Engl.* **26**, 972 (1987).
14. P. Dabo, A. Cyr, J. Lessard, L. Brossard, H. Ménard, *Can. J. Chem.* **77**, 1225 (1999).
15. Stoichiometric hydrogenolysis of aromatic C-O bond in a palladium pincer complex was reported in (*32*).
16. P. J. Dyson, *Dalton Trans.* 2964 (2003).
17. E. Wenkert, E. L. Michelotti, C. S. Swindell, *J. Am. Chem. Soc.* **101**, 2246 (1979).
18. E. Wenkert, E. L. Michelotti, C. S. Swindell, M. Tingoli, *J. Org. Chem.* **49**, 4894 (1984).
19. J. W. Dankwardt, *Angew. Chem. Int. Ed.* **43**, 2428 (2004).
20. B. T. Guan et al., *Chem. Commun. (Camb.)* 1437 (2008).
21. M. Tobisu, T. Shimasaki, N. Chatani, *Angew. Chem. Int. Ed.* **47**, 4866 (2008).
22. J. A. Widegren, R. G. Finke, *J. Mol. Catal. A* **198**, 317 (2003).
23. Materials and methods are available as supporting material on *Science* Online.
24. We observed formation of cyclohexane and cyclohexene in the reaction of Ni(COD)₂ and PCy₃ with H₂ in the absence of diphenyl ether under the same conditions (*23*).
25. F. Glorius, *Top. Organomet. Chem.* **21**, 1 (2007).
26. S. Díez-González, N. Marion, S. P. Nolan, *Chem. Rev.* **109**, 3612 (2009).
27. Ni(COD)₂ and PCy₃ were reported to catalyze silane-induced cleavage of polycyclic aromatic ethers (methoxynaphthalenes) and alkyl aryl ethers containing directing groups ortho to the C-O bond (*33, 34*).
28. No reaction was observed in the absence of Ni(COD)₂, as shown through control experiments on the cleavage of 4-tert-butylbenzyl methyl ether with hydrogen in the presence of AlMe₃ (1 equiv.), SIPr·HCl (0.4 equiv.), and NaO^tBu (2.5 equiv.) in *m*-xylene at 120°C for 32 hours (*23*).
29. For example, heterogeneous hydrogenolysis of alkyl benzyl ethers proceeds selectively in the presence of diaryl ethers over Pd(OH)₂/C (*35*).
30. K. Poppius, *Acta Chem. Scand. B* **38**, 611 (1984).
31. V. Snieckus, *Chem. Rev.* **90**, 879 (1990).
32. M. E. van der Boom, S. Y. Liou, Y. Ben-David, L. J. W. Shimon, D. Milstein, *J. Am. Chem. Soc.* **120**, 6531 (1998).
33. P. Álvarez-Bercedo, R. Martin, *J. Am. Chem. Soc.* **132**, 17352 (2010).
34. M. Tobisu, K. Yamakawa, T. Shimasaki, N. Chatani, *Chem. Commun.* Published online 24 January 2011 (10.1039/c0cc05169a).
35. B. A. Ellsworth et al., *Bioorg. Med. Chem. Lett.* **18**, 4770 (2008).
36. We thank the BP for financial support of this project through the Energy Biosciences Program and T. Rauchfuss for helpful discussions. A provisional patent has been filed on the methods presented herein.

High-Performance Electrocatalysts for Oxygen Reduction Derived from Polyaniline, Iron, and Cobalt

Gang Wu,[1] Karren L. More,[2] Christina M. Johnston,[1] Piotr Zelenay[1]*

The prohibitive cost of platinum for catalyzing the cathodic oxygen reduction reaction (ORR) has hampered the widespread use of polymer electrolyte fuel cells. We describe a family of non–precious metal catalysts that approach the performance of platinum-based systems at a cost sustainable for high-power fuel cell applications, possibly including automotive power. The approach uses polyaniline as a precursor to a carbon-nitrogen template for high-temperature synthesis of catalysts incorporating iron and cobalt. The most active materials in the group catalyze the ORR at potentials within ~60 millivolts of that delivered by state-of-the-art carbon-supported platinum, combining their high activity with remarkable performance stability for non–precious metal catalysts (700 hours at a fuel cell voltage of 0.4 volts) as well as excellent four-electron selectivity (hydrogen peroxide yield <1.0%).

Thanks to the high energy yield and low environmental impact of hydrogen oxidation, the polymer electrolyte fuel cell (PEFC) represents one of the most promising energy conversion technologies available today. Of the many possible applications, ranging from sub-watt remote sensors to residential power generators in excess of 100 kW, automotive transportation is especially attractive. PEFCs promise major improvements over gasoline combustion, including better overall fuel efficiency and reduction in emissions (including CO₂). The spectacular progress in fuel cell technology notwithstanding, a large-scale market introduction of fuel cell–powered vehicles continues to face various challenges, such as the lack of hydrogen infrastructure and the technical issues associated with PEFC performance and durability under the operating conditions of an automotive power plant. The high cost of producing PEFCs represents the most formidable challenge and has driven much of the applied and fundamental fuel cell research in recent years.

According to the latest cost analysis, the fuel cell—more precisely, the fuel cell stack—is responsible for more than 50% of the PEFC power system cost (*1, 2*). Although a state-of-the-art PEFC stack uses several high-priced components, the catalysts are by far the most expensive constituent, accounting for more than half of the stack cost. Because catalysts at both the fuel cell anode and cathode are based on platinum (Pt) or platinum alloys, their cost is directly linked to the price of Pt in the volatile and highly monopolized precious metal market. The precious metal catalyst is the only fuel cell stack component that will not benefit from economies of scale, and an increase in the demand for fuel cell power systems is bound to drive up the already high price of Pt, about $1830 per troy ounce at present ($2280 per troy ounce at its maximum in March 2008) (*3*). Thus, PEFCs are in need of efficient, durable, and inexpensive alternatives to Pt and Pt-based catalysts.

Ideally, Pt should be replaced at both fuel cell electrodes; however, its substitution at the cathode with a non–precious metal catalyst would have comparatively greater impact, because the slow oxygen reduction reaction (ORR) at this electrode requires much more Pt than the faster hydrogen oxidation at the anode. As a consequence, the development of non–precious metal catalysts with high ORR activity has recently become a major focus of PEFC research (*4–8*). The Pt replacement candidates that have attracted the most attention have been synthesized by heating precursors comprising nitrogen, carbon, and geologically abundant transition metals, iron and cobalt (M = Co and/or Fe) in particular (*9–14*). Although the nature of the active ORR catalytic sites in such N-M-C catalysts continues to be at the center of an ongoing debate (*6, 7, 10, 15*), there is no doubt that the ORR performance of N-M-C catalysts strongly depends on the type of nitrogen and transition-metal precursors used, heat treatment temperature, carbon support morphology, and synthesis conditions.

We recently initiated a research effort to develop non–precious metal catalysts that combine high ORR activity with good performance stability, originally concentrating on materials obtained without heat treatment. The polypyrrole (PPy)-Co-C system prepared this way showed respectable performance durability for a non–precious metal

[1]Materials Physics and Applications Division, Los Alamos National Laboratory, Los Alamos, NM 87545, USA. [2]Materials Science and Technology Division, Oak Ridge National Laboratory, Oak Ridge, TN 37831, USA.

*To whom correspondence should be addressed. E-mail: zelenay@lanl.gov

ERRATUM

Reports: "Selective, nickel-catalyzed hydrogenolysis of aryl ethers" by A. G. Sergeev and J. F. Hartwig (22 April, p. 439). There were two errors introduced during proofs. The third sentence of the first paragraph should read, "In addition, brown coal's polymeric network contains aromatic C-O bonds inherited from lignocellulosic biomass, and the hydrogenolysis of these bonds could facilitate the liquefaction of this carbon source and its conversion to arene feedstocks (*6*)." The last sentence of the last paragraph should read, "Although these mechanistic issues have yet to be resolved, and turnover numbers of the catalyst must be improved, the results from this work have demonstrated that the selective cleavage of aromatic C-O bonds in the presence of aliphatic C-O bonds can be conducted without reduction of the arene units by using a widely available metal and the cheap, mild, and atom-economical reductant hydrogen."

Science

Selective, Nickel-Catalyzed Hydrogenolysis of Aryl Ethers

Alexey G. Sergeev and John F. Hartwig

ARTICLE TOOLS	http://science.sciencemag.org/content/332/6028/439
SUPPLEMENTARY MATERIALS	http://science.sciencemag.org/content/suppl/2011/04/20/332.6028.439.DC1
RELATED CONTENT	http://science.sciencemag.org/content/sci/332/6035/1263.4.full
REFERENCES	This article cites 27 articles, 1 of which you can access for free http://science.sciencemag.org/content/332/6028/439#BIBL
PERMISSIONS	http://www.sciencemag.org/help/reprints-and-permissions

Use of this article is subject to the Terms of Service